

**Accurate evaluation of Einstein's A and B
coefficients of rovibrational transitions for
carbon monoxide:
Spectral simulation of $\Delta v = 2$ rovibrational
transitions in the solar atmosphere observed
by a satellite**

Kazutoshi Okada ^{a,b,c}, Mutsumi Aoyagi ^a
and Suehiro Iwata ^{a,d,1}

^a*Institute for Molecular Science, Okazaki 444-8585*

^b*Graduate University for Advanced Studies, Okazaki 444-8585*

^c*Japan Science and Technology Corporation, Chiyoda, Tokyo 108-0021*

^d*Graduate School of Science, Hiroshima University, Higashi-Hiroshima, 739-8526,
Japan*

Abstract

Accurate potential energy and dipole moment curves of the ground state carbon monoxide CO were calculated with the multi-reference configuration interaction method. Vibrational and spectroscopic constants were determined and compared with the values derived from experimental data. Einstein's A and B coefficients of the rovibronic transitions of $\Delta v = 1, 2$ and 3 were evaluated. The near-infrared absorption spectra in the solar atmosphere observed by a satellite were simulated with the calculated rovibronic transitions and the temperature of the gas was estimated around 5000 to 5500K.

Key words: Carbon monoxide, rovibrational spectra, Einstein's A and B coefficients, sun atmosphere

¹ To whom the correspondence should be sent.
e-mail address: iwata@ims.ac.jp

Introduction

Carbon monoxide (CO) molecule is one of the most important diatomic molecules in atmospheric chemistry of our earth and of some of planets in the solar system. The molecule also exists in the atmosphere of the sun itself. Carbon monoxide is one of the most extensively studied in interstellar chemistry. There are numerous studies on the vibrational and rotational spectroscopies of the ground $X^1\Sigma_g^+$ state. Recently, with an interferometric spectrometer on a satellite operated by NASA [1], the extensive and accurate infrared absorption spectra of carbon monoxide in very broad energy range were observed. The light source was the sun, and the sample gases are in the solar atmosphere. Not only the $\Delta v = 1$ bands but also the $\Delta v = 2$ and $\Delta v = 3$ bands were observed. Because of very hot environment of the solar atmosphere, the high rovibrational levels up to $v = 20$ and $J = 133$ were detected and identified. From the assigned transitions, an accurate set of Dunham coefficients were deduced, and thus the accurate potential energy curve and the rovibrational levels up to $v = 20$, which is about 45 % of the dissociation energy, were determined. But, in our knowledge, the intensity distribution of the observed spectra has not been analyzed.

There are also numerous theoretical studies on the ground $X^1\Sigma_g^+$ state of CO. For instance, the sign and value of dipole moment at the equilibrium bond distance have been one of the hot topics in the history of ab initio electronic structure theories [2]. Recently, Sundholm et al [3] calculated the potential energy and one- and two-photon dipole moment functions, vibrational spectroscopic constants and oscillator strengths. Langhoff and Baucshlicher (LB) also calculated the potential energy and dipole moment functions, and evaluated the radiative lifetime of rotationless vibrational excited levels [4]. Their theoretical studies reproduce experimental data reasonably well. However, as far as the rovibrational levels are concerned, there have been few studies that can be used for the analysis of the above mentioned spectra of the solar atmosphere both in energy and in spectral intensity.

In the present studies, we attempt more accurate calculations than the previous studies for the ground $X^1\Sigma_g^+$ state of CO. The potential energy and dipole moment functions are calculated, and the rovibrational wavefunctions on the potential energy curve up to near vibrational dissociation limit and rotational levels $J \sim 100$ are evaluated. Einstein's A and B coefficients of rovibrational transitions are evaluated using the rovibrational energies and their wavefunctions. The rovibrational infrared spectra are constructed for $\Delta v = 1, 2$ and 3 , and the calculated spectra are compared with the recent experimental data from the satellite as well as with the previous theoretical studies. By simulating the rovibrational spectra in the $\Delta v = 2$ region observed at the satellite [1], we could deduce the temperature distribution of CO molecule at the atmosphere

of sun.

1 Calculation Methods

Multireference configuration interaction (MRCI) calculations were performed for the ground state of CO. The basis set used was the augmented valence quadruple zeta (aug-ccpVQZ, AVQZ) basis set of Dunning [5]. MRCI calculations were performed with MOLPRO internally contracted CI method [6][7]. The reference configurations were all electronic configurations generated from $[1\sigma^2, 2\sigma^2, 3\sigma^{0-2}, 4\sigma^{0-2}, 1\pi^{0-4}, 5\sigma^{0-2}, 2\pi^{0-4}, 6\sigma^{0-2}, 7\sigma^{0-1}]$, where 7σ orbital is a Rydberg type orbital. The calculations were performed under C_{2v} symmetry. The valence-type vacant orbitals, 2π and 6σ , were determined by the VAL-VAC (valence-type-vacant) method of Iwata [8][9]. The method requires only a single Fock matrix generation, and provides us with a proper anti-bonding nature of molecular orbitals. The other occupied orbitals ($1\sigma - 5\sigma, 1\pi$) are the closed shell SCF orbitals. The orbital set used in the calculations are identical with that used for the low-lying states of carbon monoxide cation CO^+ [9][10].

Vibrational energies and wavefunctions on the adiabatic potential energy curve were calculated by solving the one-dimension nuclear Schrödinger equation with the FEM1D program of Kimura et al [11]. The integration region was between 1.4 and 10.0 Bohr. The energy at bond lengths between the ab initio calculated points is evaluated with the 5th order akima interpolation or with the analytical function discussed below. Vibrational spectroscopic constants ω_e , $\omega_e x_e$ and $\omega_e y_e$ were obtained using the least-squares fitting of $\Delta G_{v+1/2} = G(v+1) - G(v)$, $G(v)$ being the vibrational energy relative to the lowest vibrational level. The energy $G(v)$ is expressed as

$$G(v) = \omega_e \left(v + \frac{1}{2} \right) - \omega_e x_e \left(v + \frac{1}{2} \right)^2 + \omega_e y_e \left(v + \frac{1}{2} \right)^3 \quad (1)$$

By integrating the dipole moment function over the vibrational wavefunctions for each rotational quantum number J , Einstein's A and B coefficients of the rovibrational transitions were evaluated.

2 Results and discussion

2.1 Vibrational spectroscopic constants

Figure 1 shows potential energy and dipole moment curves of the neutral ground $X^1\Sigma_g^+$ state of CO. The thin horizontal lines on the potential energy curve are the calculated vibrational levels. The origin of energy is set to be at the calculated $v = 0$ vibrational energy level. The vertical dashed line shows the equilibrium bond length, $R = R_e$, and the horizontal dashed line shows zero permanent dipole moment. The positive sign of dipole moment represents C^+O^- . At $R = R_e$, the sign of the dipole moment of the molecule is slightly negative as has been known in the previous studies [2]. As the bond length increases, the dipole moment becomes positive; the molecule is polarized as $\text{C}^{\delta+}\text{O}^{\delta-}$. At $R \sim 1.90 \text{ \AA}$, the dipole moment has a maximum positive value. At near dissociation limit, the dipole moment asymptotically becomes zero.

Langhoff and Bauschlicher(LB) reported both potential energy and dipole moment curves with the then state-of-art level of calculations[4]. To estimate the accuracy of calculated potential energy and dipole moment functions, the spectroscopic constants R_e , D_e , ω_e , $\omega_e x_e$ and $\omega_e y_e$ are calculated using the functions of ours and LB's. The calculated spectroscopic constants are compared with the available experimental data in Table 1.

Figure 2 shows the spacings between adjacent vibrational levels, $\Delta G_{v+1/2}(v) = G(v+1) - G(v) = \omega_e - 2\omega_e x_e(v+1)$, plotted against $(v+1/2)$. Experimental $\Delta G_{v+1/2}(v)$ plots in the figure are evaluated with a set of Dunham coefficients determined by the spectroscopic studies of solar carbon monoxide[1]. The vibrational spectroscopic constants ω_e , $\omega_e x_e$ and $\omega_e y_e$ are obtained using the least-squares fitting to eq. (1) below $v = 25$. The calculated plots of ours and LB's agree with the experimental data. The LB plot underestimate ω_e by about 10 cm^{-1} . In the present calculation, the error of ω_e is 2 cm^{-1} . To demonstrate the behavior of higher order anharmonicity, the spacing of $\Delta G(v)$, $\Delta\Delta G = \Delta G(v+1) - \Delta G(v)$, which is $-2\omega_e x_e + 6\omega_e y_e(v+3/2)$ in the 3rd order Dunham expansion, is shown in Figure 3. The plots $\Delta\Delta G$ used the LB results show a large oscillatory behavior, so that the plots are not included in the figure. Our calculated $\Delta\Delta G(v)$ plots also have many zigzags for $v \leq 40$. It turned out the fit $\Delta\Delta G$ is very sensitive to the potential energy functions used in solving the nuclear Schrodinger equation. In the present study we have used the 5th order Akima method in interpolating the potential energy. When a vibrational eigenvalue hits at the interpolating point, it deviates from the appropriate value. The analytical fitting is desired to obviate the zigzags in the higher order plot (see below).

As is seen from the table, the present calculations for the parameters are in very good agreement with the experiments.

2.2 Analytical potential energy function

The calculated potential energy curve shown in Fig. 1 is fitted into an analytical function. The accurate analytical form of potential energy function for any desired bond length is required for many applications in quantum chemistry. In the present study, the extended Rydberg function,

$$V_{ER}(R) = -D_e(1 + \sum_{k=1}^n a_k \rho^k) \exp(-\gamma\rho) \quad (2)$$

is used in the fitting where

$$\rho = (R_e - R)/R_e \quad (3)$$

For the polynomial part, $n = 6$ and 8 are used. The weight in the fitting

$w_i = \exp(-(V_{cal}(R_i) - V_{cal}(R_e)) / 0.1)$
is used.

Table 2 shows the determined parameters. To show the accuracy of the function, $\Delta\Delta G(v) = \Delta G(v+1) - \Delta G(v)$ obtained with the fitted function is also shown in Fig. 3. Both calculated $\Delta\Delta G(v)$ are in good agreement with experimental data. As expected, the zigzags, found when the interpolation is used, disappears in the plots. The eigenvalue is very sensible, when the turning points of the wavefunction hit at the interpolated point. By using the analytical fitted function, the smooth and consistent potential energy curve is obtained. This example is a clear warning for using the interpolation methods when the higher order spectroscopic properties are evaluated. The plots $\Delta\Delta G(v)$ of the analytical functions suggest that a slight modification of the present functions may provide an accurate potential energy curve of the ground state of carbon monoxide.

2.3 Einstein's A and B coefficients

Figure 4 shows calculated Einstein's A coefficients of rotationless vibrational transition $v'' \leftarrow v'$ of $\Delta v = v' - v'' = 1, 2$ and 3 , plotted against v'' . Langhoff

and Bauschlicher also calculated Einstein's A coefficients, and so both calculated results are compared. Both results are in very good agreement with each other. It is expected that the present calculated results are more accurate for higher v . An Einstein's A coefficient can be compared with the experimentally obtained lifetime of vibrationally excited states $v = 1$. The experimentally observed lifetime of the transition ($v'' = 0 \leftarrow v' = 1$) is 33 milliseconds; the corresponding Einstein's A coefficient is 30 s^{-1} [12]. Both calculated results agree well with the experimental value. It should be noted that the A coefficient for $\Delta v = 2$ monotonically increases with v , and becomes comparable with that for $\Delta v = 1$ at $v = 30$. To estimate the radiative decay rate for higher vibrational levels under hot environment, the $\Delta v = 2$ and 3 transitions cannot be neglected.

Figure 5 shows the vibrational quantum number (v) dependence of the calculated Einstein B coefficients of rotationless vibrational transitions $v' \leftarrow v''$ of $\Delta v = v' - v'' = 1, 2$ and 3 , plotted against v'' . For $\Delta v = 1, 2$ and 3 , Einstein's B coefficients peak at $v'' = 33, 54$ and 58 , respectively. For $\Delta v = 2$ and 3 transitions, Einstein's B coefficients are substantially large at high vibrational levels.

Large coefficients of A and B for higher vibrational levels reflect the functional form of the dipole moment shown in Fig.1. Figure 5 clearly indicates that the absorption bands for $\Delta v = 2$ and 3 are substantially strong. As is shown below, the $\Delta v = 2$ ($v' = 2 \leftarrow v'' = 0$) transitions are observed between 4250 cm^{-1} and 4360 cm^{-1} in the solar spectra. Because this wavenumber region has less absorption bands from the other molecules than the fundamental ($\Delta v = 1$) region, the measurement of the absorption bands $\Delta v = 2$ might be a good tool for monitoring the carbon monoxide in the atmospheres.

Figure 6 shows the rotational quantum number J dependence of calculated Einstein's B coefficients for some rovibrational transitions of $\Delta v = 1$ and 2 for $\Delta J = +1$ (R-branch) and $\Delta J = -1$ (P-branch). For a given $v' \leftarrow v''$ transition of $\Delta v = 1$, Einstein's B coefficients of $\Delta J = +1$ are larger than $\Delta J = -1$ for low J'' , and both coefficients become nearly equal to each other and constant for high J'' . For a given $v' \leftarrow v''$ transition of $\Delta v = 2$, on the other hand, Einstein's B coefficients of $\Delta J = +1$ are substantially larger than $\Delta J = -1$ for all J'' . Interestingly, at $J'' = 10$, the B coefficient for $\Delta J = +1$ transition is at the minimum, and that for $\Delta J = -1$ transition is at the maximum. For high J'' , Einstein's B coefficients of $\Delta J = +1$ become extremely large for $\Delta v = 2$ and 3 . The intensity ratio of the R and P branch is given as

$$\frac{R(J'' + 1; v' \leftarrow J'', v'')}{P(J'' - 1; v' \leftarrow J'', v'')} = \frac{J'' + 1}{J''} \times \frac{|\langle \chi(v'; J'' + 1) | \mu(\mathbf{R}) | \chi(v''; J'') \rangle|^2}{|\langle \chi(v'; J'' - 1) | \mu(\mathbf{R}) | \chi(v''; J'') \rangle|^2}, \quad (4)$$

where $\chi(v; J)$ is the nuclear vibrational wavefunction and $\mu(\mathbf{R})$ is the dipole moment operator. Equation (4) implies that the strong J dependence of B coefficients at high J in $\Delta v = 2$ and 3 transitions results from the J dependence of matrix elements; the J dependence of the nuclear vibrational wavefunctions has to be taken into account.

2.4 Temperature distribution of CO molecule at the solar atmosphere

With Einstein's B coefficients at hand, if the abundance of rovibrational levels (v'', J'') is known or assumed, the rovibrational absorption spectra can be simulated. In turn, if the rovibrational spectra are observed, the population of the rovibronic levels can be deduced. Based on the calculated Einstein's B coefficients of rovibrational transitions, the wide range of spectrum of the solar atmosphere can be analyzed. We assume the thermal equilibrium among the rovibrational levels; the number of molecules in the rovibrational levels is assumed to be Boltzmann distribution. The theoretical absorption spectral intensity distribution $I(v', J' \leftarrow v'', J'')$ can be evaluated by the following formulae;

$$I(v', J' \leftarrow v'', J'') = \frac{B(v', J' \leftarrow v'', J'') \times \exp(-\Delta E_{\text{vib}}/kT_{\text{vib}}) \times (2J'' + 1) \exp(-\Delta E_{\text{rot}}/kT_{\text{rot}})}{\sum_{v'', J''} \exp(-\Delta E_{\text{vib}}/kT_{\text{vib}}) \times (2J'' + 1) \exp(-\Delta E_{\text{rot}}/kT_{\text{rot}})} \quad (5)$$

$$\Delta E_{\text{vib}} = E(v', 0) - E(v'', 0)$$

$$\Delta E_{\text{rot}} = E(v'', J') - E(v'', J'')$$

where $B(v', J' \leftarrow v'', J'')$ is Einstein's B coefficient of the rovibrational transition $(v', J' \leftarrow v'', J'')$ and T_{vib} (T_{rot}) is vibrational (rotational) temperature. In the present simulation $T_{\text{vib}} = T_{\text{rot}}$ is assumed.

Figure 7 shows the simulated and experimentally observed absorption spectra between 4250 cm^{-1} and 4370 cm^{-1} , where the transitions $v' = 2 \leftarrow v'' = 0$ and $v' = 3 \leftarrow v'' = 1$ are observed. In the simulation the maximum J'' is 83, and the band head is at $J'' = 50$. The background in the reported data [13] is subtracted to compare the observed spectrum with the simulated one. In Fig. 7 the assumed temperature is 5000 K . The simulated spectrum is uniformly shifted downward by 7 cm^{-1} . Note that no adjustable parameters other than 7 cm^{-1} shift and the temperature are used in the simulation. The simulated spectrum well reproduces the observed spectrum. We have also attempted the theoretical absorption spectra for $\Delta v = 1$ and compared them with the solar spectra. Because the spectra range is around 2200 cm^{-1} , there are strong and irregular background absorption bands. Therefore, without the proper

subtraction of the background, the simulated spectra cannot be compared with the observed ones.

Both the experimentally observed and the calculated absorption intensities $I(v', J' \leftarrow v'', J'')$ for $\Delta v = 2$ are well fitted to an analytical function

$$I(J'' + 1 \leftarrow J'', v' = v'' + 2 \leftarrow v'') = (a + b \times J'') \exp(-c \times J''^2) \quad (6)$$

with three parameters a, b and c . The parameters are given in Table 3, which might be used in the detailed analysis of the spectra. Figure 8 shows the simulated and experimentally observed absorption intensities of rovibrational spectra for $v' = 2 \leftarrow v'' = 0$; $\Delta J = +1$ and for $v' = 4 \leftarrow v'' = 2$; $\Delta J = +1$, plotted against J'' . The experimentally obtained intensity [13] is superimposed on the simulated results with the assumed temperatures between 4000 K and 6000 K with 500 K interval. Both Table 3 and Figure 8 indicate that the temperature of carbon monoxide molecules of the solar atmosphere distributes between 4500 K and 5500 K . The distribution of temperature of carbon monoxide molecules on the sun may suggest the altitude range where the gas exists.

2.5 Concluding remarks

With the accurate potential energy and dipole moment curves and rovibrational wavefunctions on the potential energy curve, Einstein's A and B coefficients are evaluated. The calculated spectroscopic constants and Einstein's coefficients quantitatively reproduce the experimental data, if they ever exist.

With the quantitatively reproduced calculated results, the simulation of rovibrational absorption spectra are performed. The simulated absorption spectra are compared with the experimental absorption spectra from the solar atmosphere. The vibrational and rotational temperatures of solar atmosphere are estimated. The vibrational and rotational temperatures of the carbon monoxide gas in the solar atmosphere are estimated to lie between 4500 K and 5500 K .

The tables of A and B coefficients as well as the raw data of the potential energy and dipole moment functions are distributed through the web site (http://hera.chem.sci.hiroshima-u.ac.jp/iwata_home/index.html).

The work is partially supported by the Grant-in-Aids for Science Research (No. 11166270 and 11640518) by the Ministry of Education, sports, and Cul-

ture, Japan, and by the project 'Computational Chemistry of Molecules in the Atmospheric Environment' of Research and Development Applying Advanced Computational Science and technology under Japan Science and Technology Corporation.

References

- [1] R. Furrenq, G. Guelachvili, A.J. Sauval, N. Grevesse and C. B. Farmer, *J. Mol. Spectr.*, **149** (1991) 375.
- [2] F. Grimaldi, A. Lecourt, and C. Moser, *Int. J. Quant. Chem.*, **S1** (1967) 153.
- [3] D. Sundholm, J. Olsen and P. Jørgensen, *J. Chem. Phys.*, **102** (1995) 4143.
- [4] S. R. Langhoff and C. W. Bauschlicher, Jr., *J. Chem. Phys.*, **102** (1995) 5220.
- [5] T. H. Dunning Jr, *J. Chem. Phys.*, **90** (1989) 1007.
- [6] H. -J. Werner and P. J. Knowles, *J. Chem. Phys.*, **89** (1988) 5803.
- [7] P. J. Knowles and H. -J. Werner, *Chem. Phys. Lett.*, **145** (1988) 514.
- [8] S. Iwata, *Chem. Phys. Lett.*, **83** (1981) 134.
- [9] K. Okada and S. Iwata, *J. Electr. Spectr. Related Topics*, **108** (2000) 225
- [10] K. Okada and S. Iwata, *J. Chem. Phys.* **112** (2000) 1804.
- [11] T. Kimura, N. Sato, and S. Iwata, *J. Comp. Chem.*, **9** (1988) 827.
- [12] R. C. Millikan. *J. Chem. Phys.*, **38** (1963) 2855.
- [13] http://nssdc.gsfc.nasa.gov/space/model/sun/ir_spectrum.html
- [14] K. P. Huber and G. Herberg, *Constants of Diatomic Molecules*, (Van Nostrand Reinhold Co., New York, 1979)

Figure Caption

Figure 1. The potential energy and dipole moment curves of the ground $X^1\Sigma^+$ state. The positive sign of the dipole moment curve implies $O^{6+}O^{6-}$.

Figure 2. The spacings between adjacent vibrational levels, $\Delta G_{v+1/2}(v) = G(v+1) - G(v)$, plotted against $(v+1/2)$. The lines are the least square fitted to equation (1). ■ The energy evaluated with the Dunham coefficients [1]. ○ The present results. ● The energy evaluated using the potential energy curve reported by reference [4].

Figure 3. The spacings of $\Delta G(v)$, $\Delta\Delta G = \Delta G(v+1) - \Delta G(v)$, plotted against v .

■ The energy evaluated with the Dunham coefficients [1]. ● The potential energy was evaluated by using the akima interpolation formula when the nuclear Schrödinger equation is solved. ○ The potential energy function (2) of the 8th order. □ The potential energy function (2) of the 6th order.

Figure 4 Calculated Einstein's A coefficient of rotationless vibrational transition $v'' \leftarrow v'$ of $\Delta v = v' - v'' = 1, 2$ and 3 , plotted against v'' . ○ reference [4].

Figure 5 Calculated Einstein's B coefficient of rotationless vibrational transition $v' \leftarrow v''$ of $\Delta v = v' - v'' = 1, 2$ and 3 , plotted against v'' .

Figure 6. The rotational quantum number (J) dependence of the calculated Einstein's B coefficients of $(v', J') \leftarrow (v'', J'')$ for some $\Delta v = 1$ and 2 transitions with $\Delta J = +1$ (R -branch) and $\Delta J = -1$ (P -branch). a) $\Delta v = 1$, b) $\Delta v = 2$.

Figure 7. The simulated and observed absorption spectra between 4250 cm^{-1} and 4370 cm^{-1} . The observed data are taken from Reference[13]. The background was subtracted in the figure.

Figure 8. The simulated J dependence of rovibrational bands $\Delta J = +1$ at $T = 4000, 4500, 5000, 5500$ and 6000 K . The intensities in the observed spectra [13] are given in the figure by ○. a) The series for $v' = 2 \leftarrow v'' = 0$. b) The series for $v' = 4 \leftarrow v'' = 2$.

Table 1 The calculated and experimental spectroscopic constants^a.

	$R_e/\text{\AA}$	ω_e/cm^{-1}	$\omega_e x_e/\text{cm}^{-1}$	$\omega_e y_e/\text{cm}^{-1}$	D_e^d/cm^{-1}
Langhoff and Bauschlicher ^b	1.132	2159.3	13.60	0.0216	85691
Present	1.130	2172.0	13.09	0.0117	90078
Experiment ^c	1.128 ^e	2170.0	13.33	0.0134	88316
		(2169.8) ^e	(13.288) ^e	(0.0105) ^e	(90551 ± 137) ^e

a) The constants, ω_e , $\omega_e x_e$ and $\omega_e y_e$, are determined by fitting the vibrational energies below $v = 25$ to equation (1).

b) The rotationless vibrational energies are evaluated from the potential energy curve given in Reference [4].

c) The rotationless vibrational energies are evaluated with the Dunham coefficients reported in Reference [1].

d) The dissociation energy is estimated by assuming the Morse function, where the constants ω_e and $\omega_e x_e$ are determined by the fitting the vibrational energies below $v = 25$.

e) Reference [14]. The constants ω_e , $\omega_e x_e$ and $\omega_e y_e$ are a part of the 6th order polynomial of $(v + 1/2)$, fitted below $v = 37$. The dissociation energy is estimated by adding to D_0 the $v = 0$ energy evaluated by the Dunham expansion. $D_e = (11.092 \pm 0.017) * 8065.54 + 1088.2 \text{ cm}^{-1}$.

Table 2 The parameters for the fitted potential energy curve to the analytical function (2).

	6th order ($n = 6$)	8th order ($n = 8$)
$D_e/\text{Hartree}$	0.410587	0.409949
D_e/cm^{-1}	90113.4	89973.4
R_e/Bohr	2.133965	2.168867
$R_e/\text{\AA}$	1.129	1.148
a_1	3.088175	3.934579
a_2	-2.127217	1.534229
a_3	2.029493	1.739583
a_4	-2.794072	-0.935014
a_5	1.425327	0.179972
a_6	-0.221847	-2.178445
a_7		1.832090
a_8		-0.375251
γ	3.079123	4.137383

Table 3 Experimentally observed and calculated absorption intensities fitted to an analytical function (6) with three parameters a , b and c .

	$I(v' = 2, J' \leftarrow v'' = 0, J'')$			$I(v', J' = 4 \leftarrow v'' = 2, J'')$		
	a	b	c	a	b	c
exp ^a	0.0047454	0.010523	4.8894E-4	0.0062029	0.021368	4.4780E-4
4000K	0.0058430	0.0032361	6.0541E-4	0.0081506	0.0045938	5.9739E-4
4500K	0.0052267	0.0025822	5.3143E-4	0.0072906	0.0036682	5.2479E-4
5000K	0.0047315	0.0020566	4.7248E-4	0.0065998	0.0029235	4.6695E-4
5500K	0.0047596	0.0017874	4.2443E-4	0.0060324	0.0023104	4.1982E-4
6000K	0.0039844	0.0012632	3.8453E-4	0.0055579	0.0017968	3.8069E-4

a) Reference [1][13]

Fig. 1

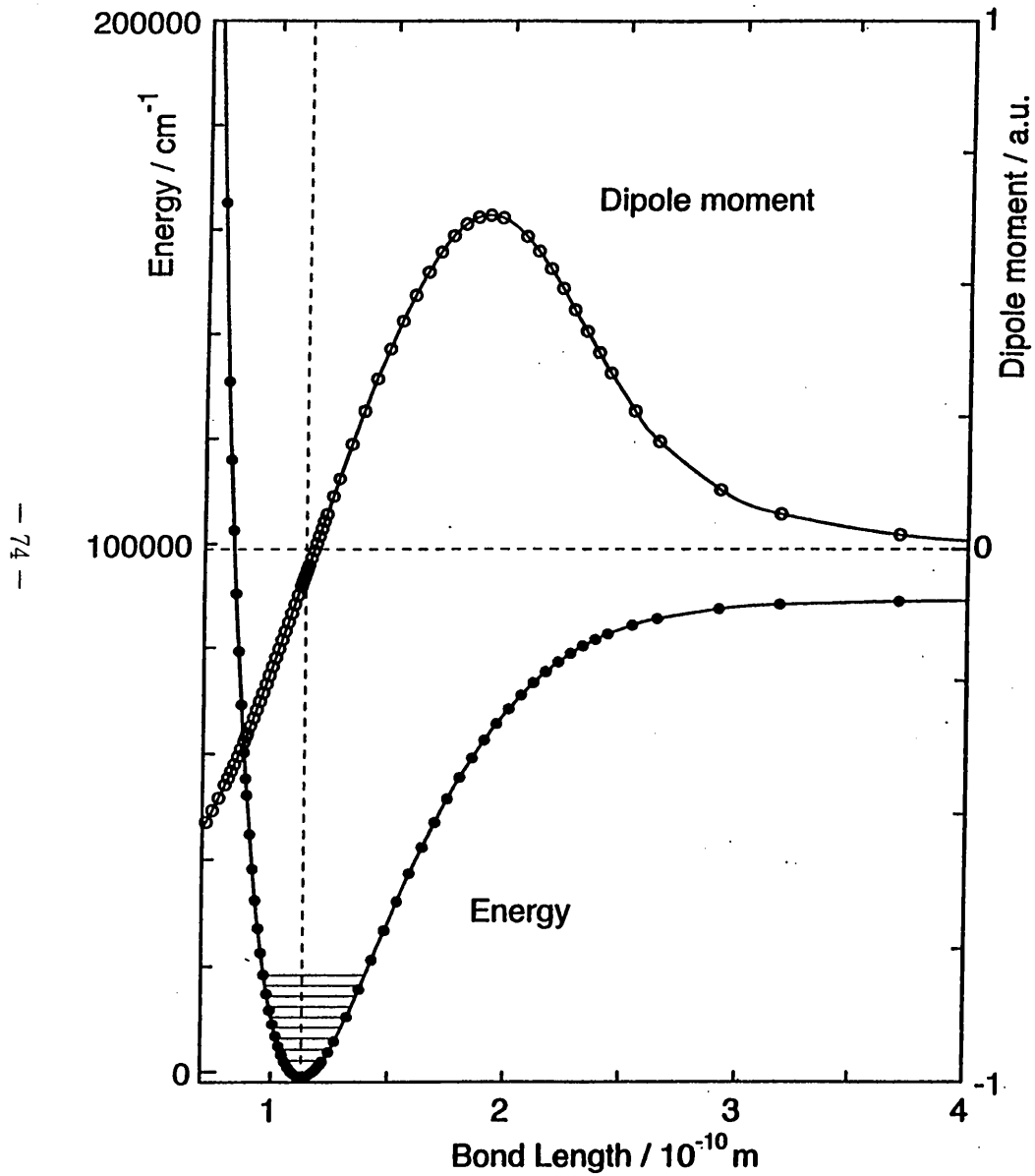


Fig. 2

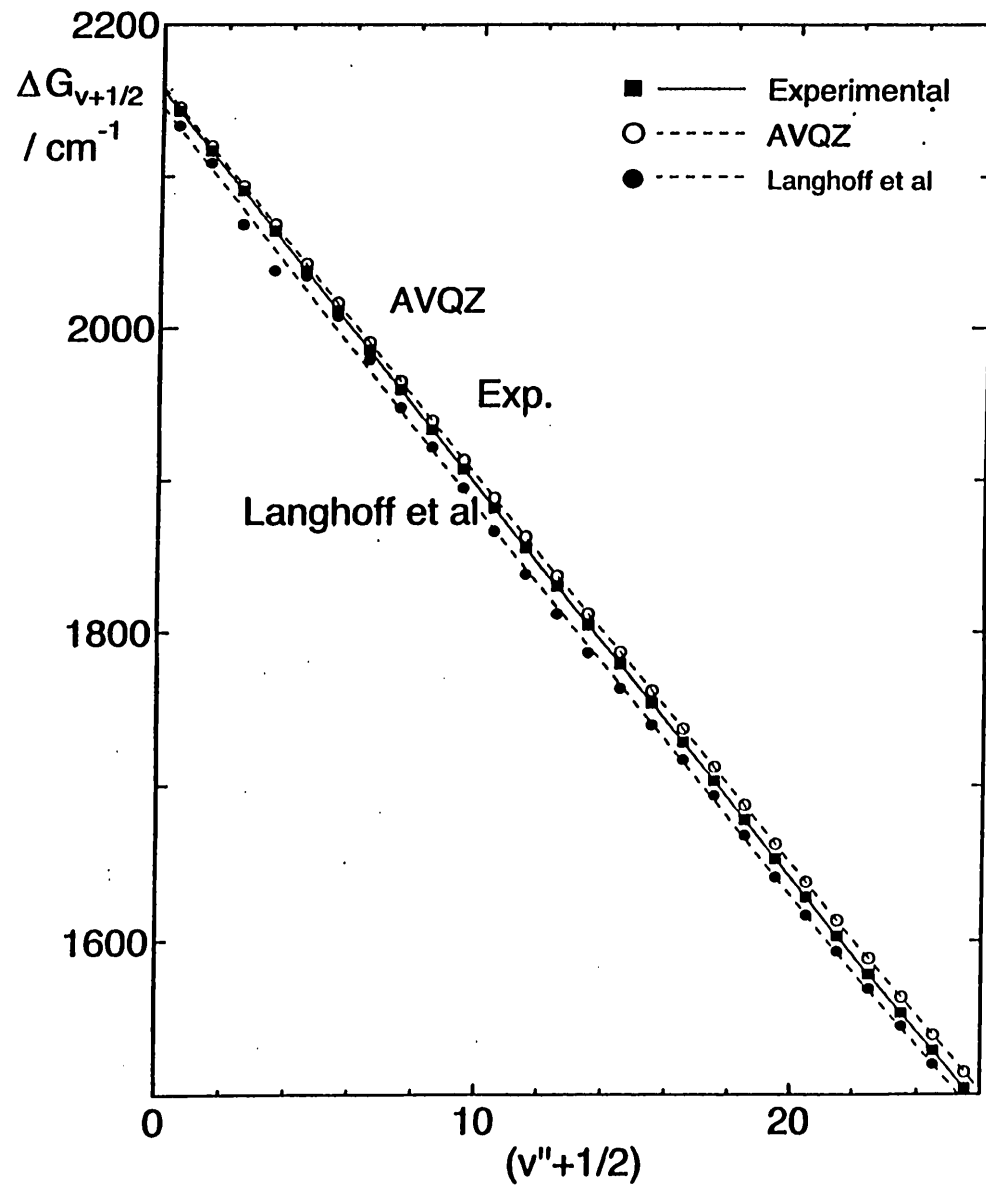
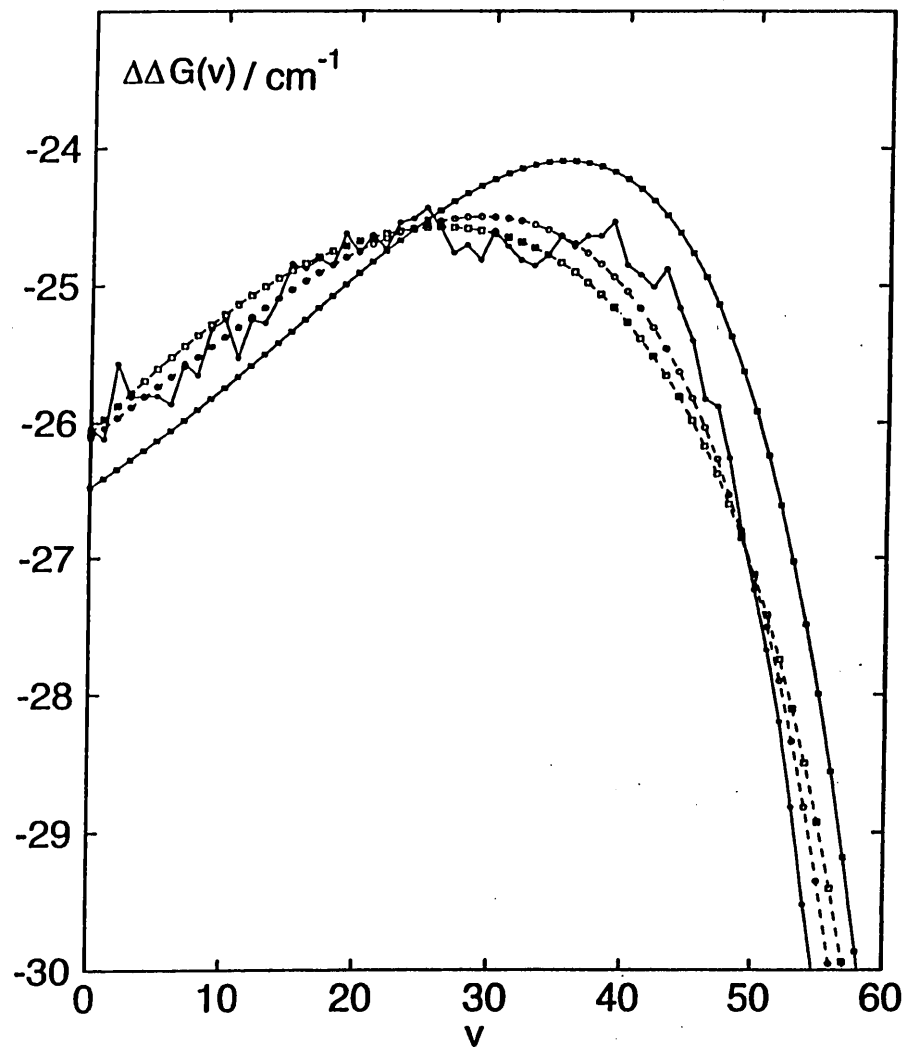


Fig. 3



- 75 -

Fig. 4

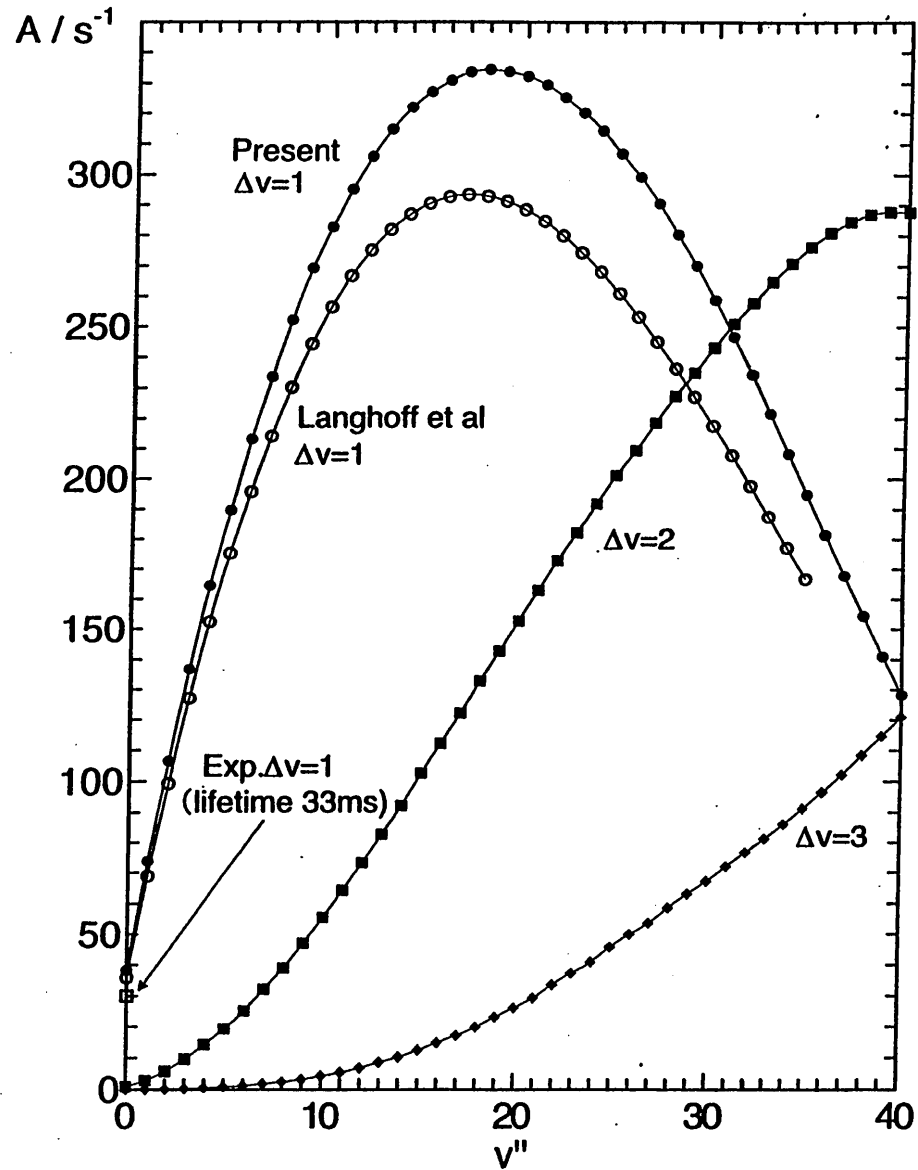


Fig. 5

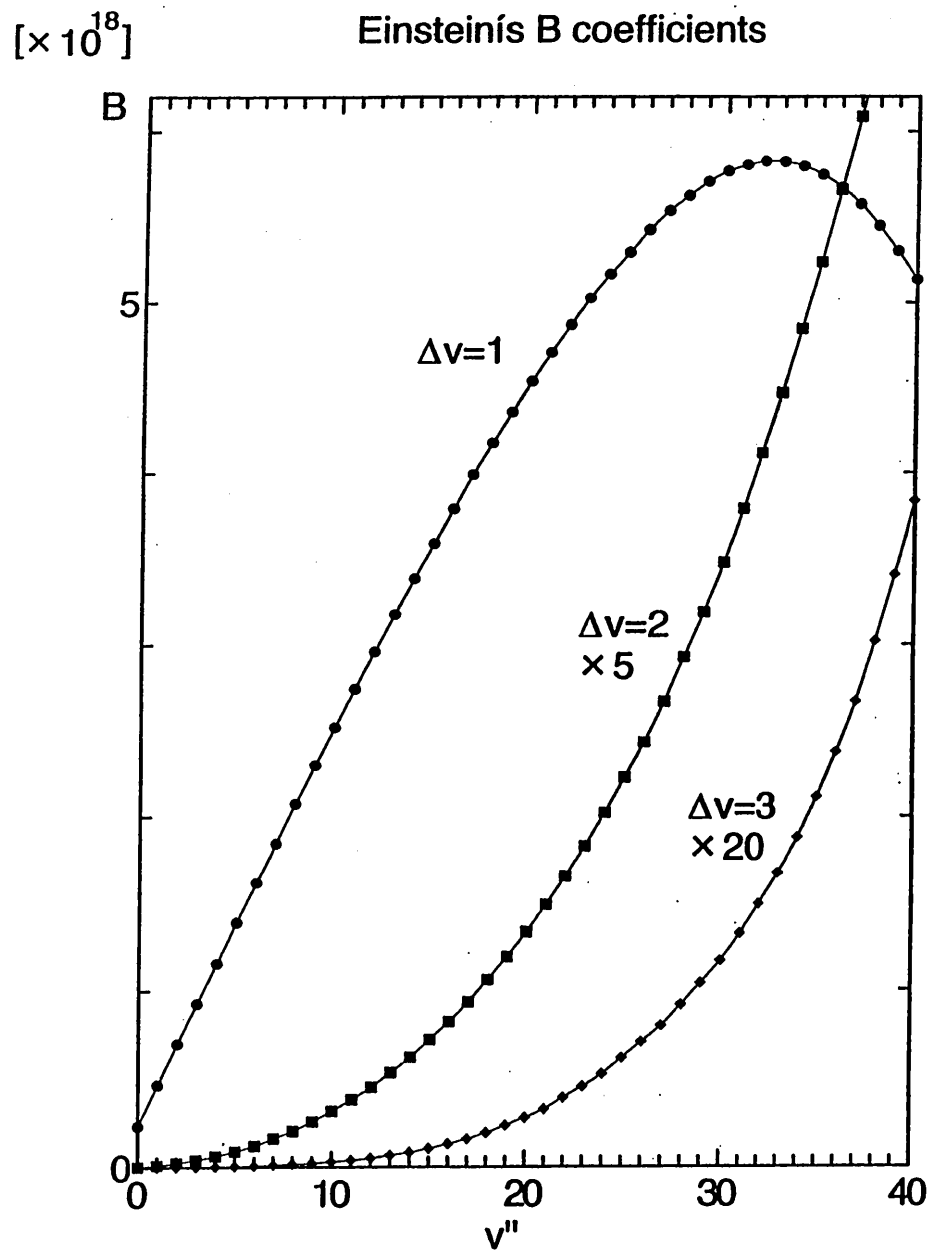


Fig. 6 (a)

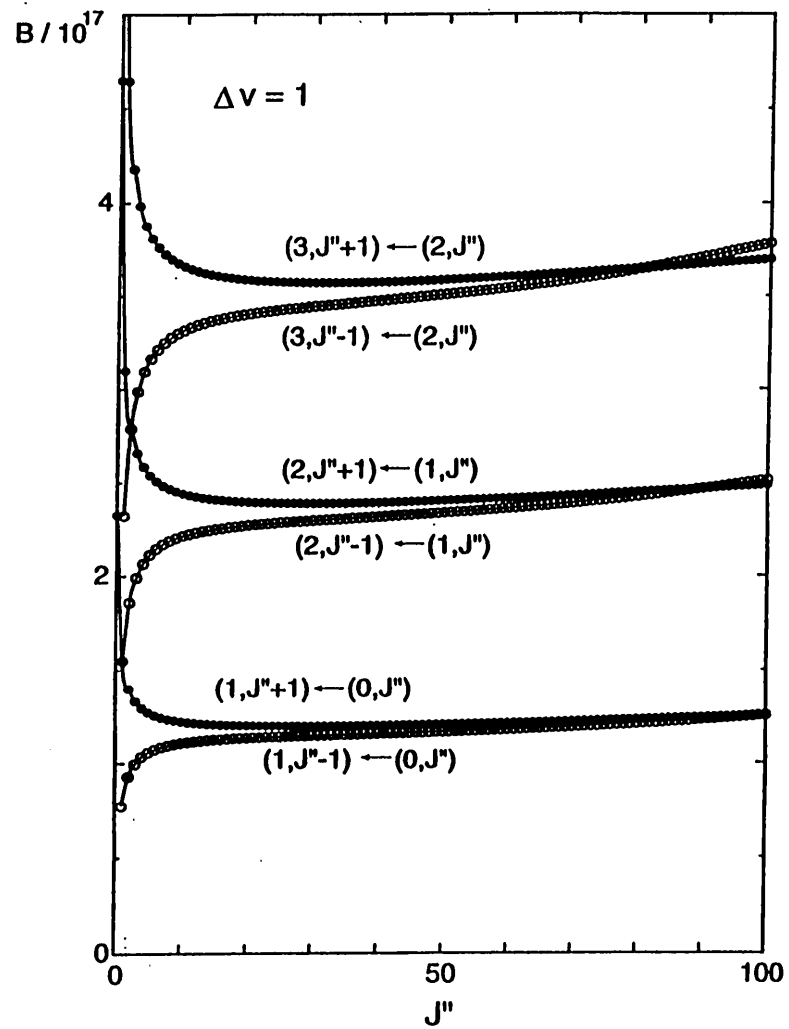
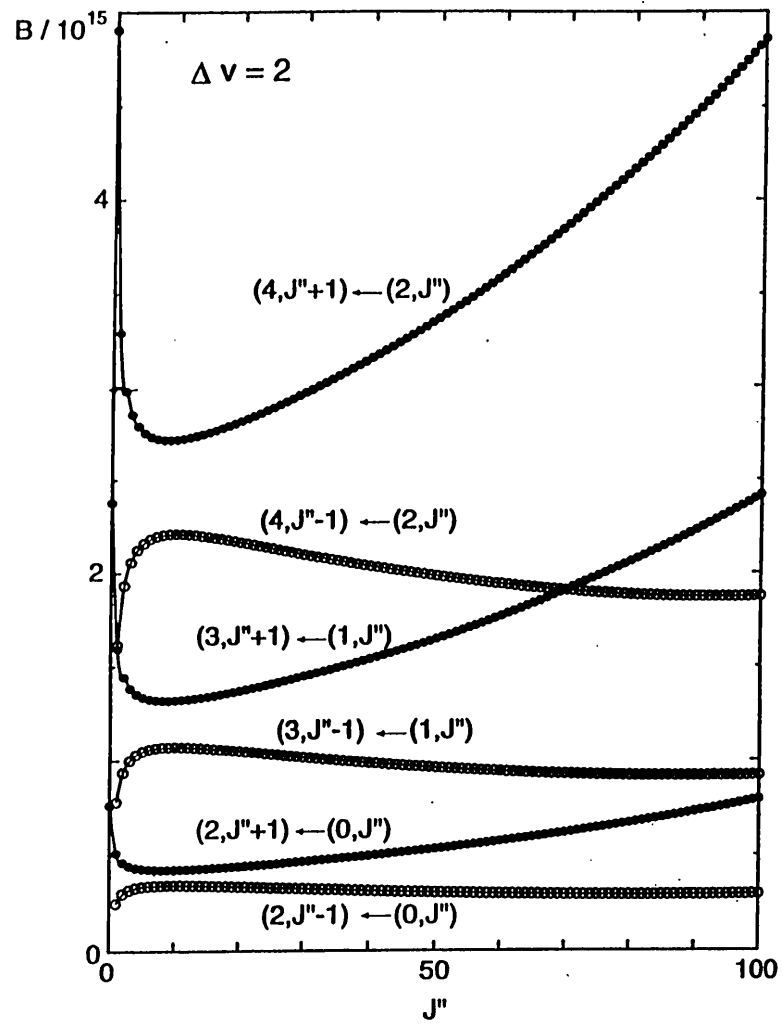


Fig. 6 (b)



- 77 -

Fig. 7

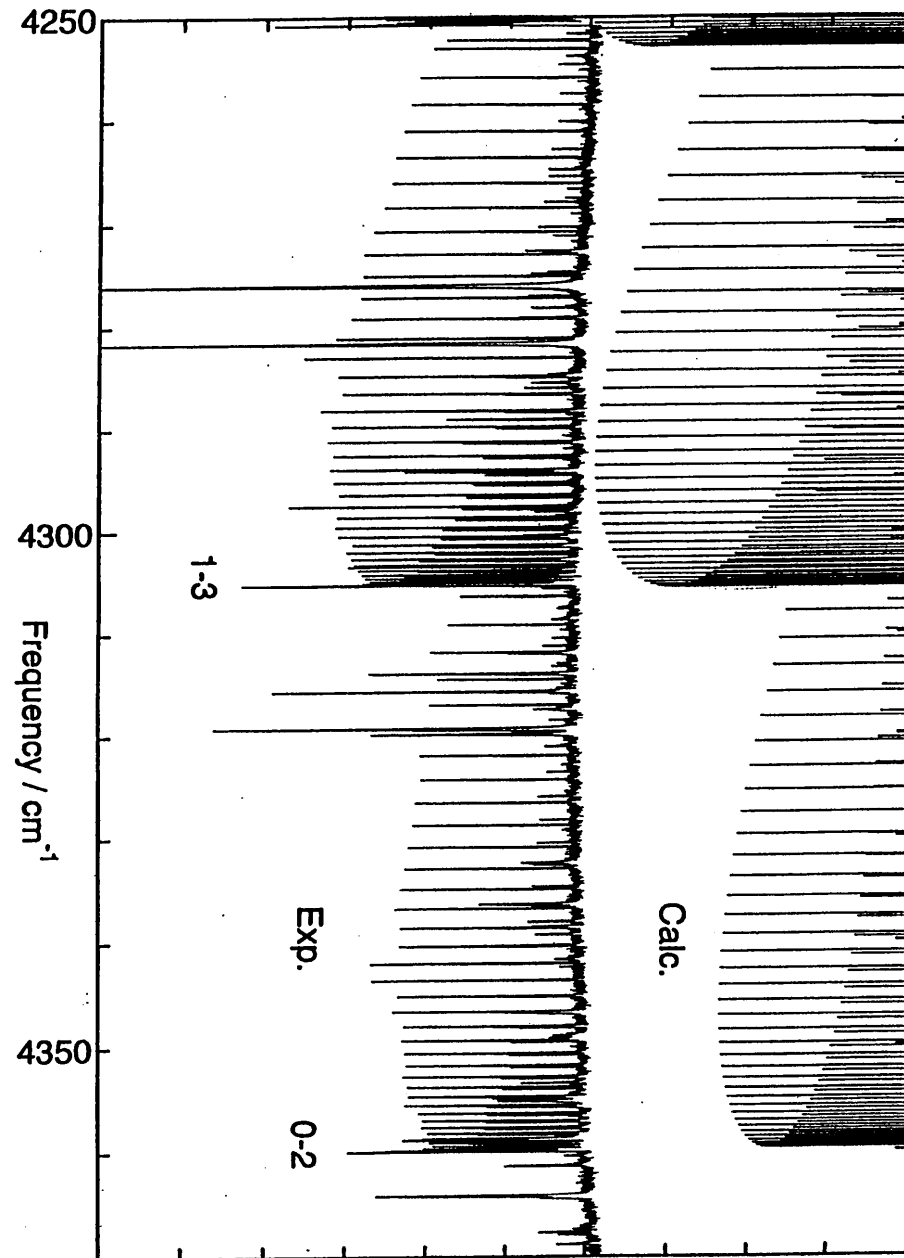


Fig. 8 (a)

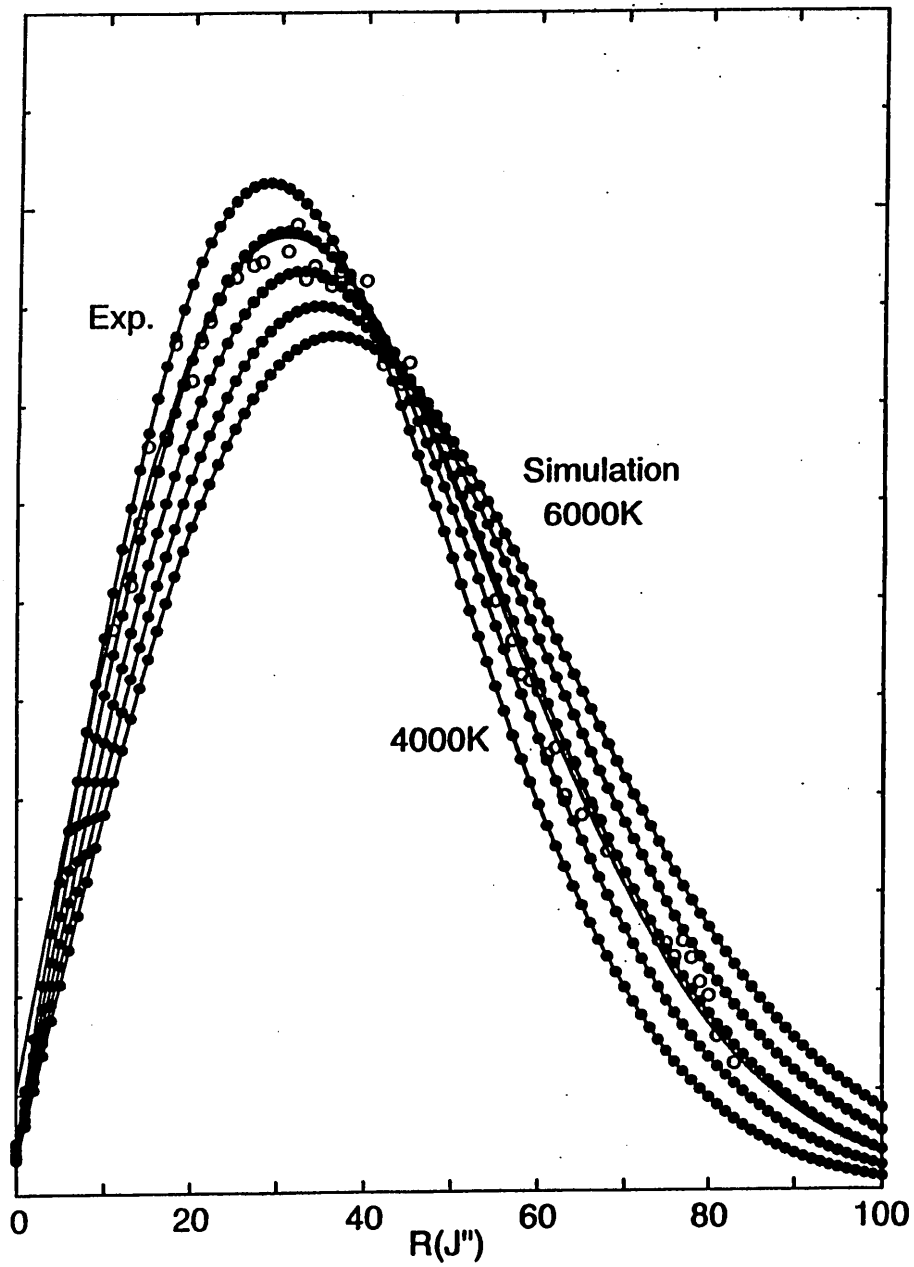


Fig. 8 (b)

